

and

$$\phi_i = \frac{1}{2}(1 + \xi\xi_i)(1 - \eta^2) \quad \text{for} \quad \eta_i = 0.$$

Corresponding cubic and Hermite bases are summarized in Table 2.7a. Bases of this class are generally referred to as serendipity basis functions.

It is interesting at this point to examine the significance of dropping the $\xi^2\eta^2$ term in formulating the interpolating polynomial (2.2.64). The quadratic and cubic serendipity bases are presented in Figure 2.12a and b and can readily be compared with the Lagrangian bases of Figure 2.11. Note that although an overall similarity exists, the Lagrangian bases are somewhat different in the interior because of the additional constraints imposed on their formulation. It can be shown, using a type of analysis to be presented later, that the addition of the $\xi^2\eta^2$ term in general has little influence on the overall accuracy of the approximation.

To this point we have tacitly assumed that one type of element, be it linear, quadratic, or cubic, would be used to represent all regions in a particular domain. There are occasions, however, where higher-degree elements may be required in one region but not another. This situation generally arises when the solution is not a smooth surface, such as in the vicinity of singularities or abrupt changes in medium properties. To change from one element type to another requires a transition element. This element must be sufficiently flexible that a different degree of basis function can be used along each side (see Figure 2.12c). The formulation of these bases is presented in Table 2.7a (Pinder and Frind, 1972).

Hermitian Basis Functions. Although the two-dimensional Hermite bases are generated through a straightforward multiplication of the one-dimensional functions of Figure 2.9, they are somewhat more difficult to apply than the C^0 continuous cubics mentioned above. The two-dimensional expansion of the trial function $\hat{T}(t)$ now contains, in general, six unknown parameters per node: T_j , $\partial T_j/\partial x$, $\partial T_j/\partial y$, $\partial^2 T_j/\partial x \partial y$, $\partial^2 T_j/\partial x^2$, and $\partial^2 T_j/\partial y^2$. For any point within an element, we obtain*

(2.2.68)

$$\begin{aligned} \hat{T} = & \sum_{j=1}^4 T_j \phi_{00j}^1 + \frac{\partial T_j}{\partial x} \phi_{10j}^1 \frac{\partial x}{\partial \xi} j + \frac{\partial T_j}{\partial x} \phi_{01j}^1 \frac{\partial x}{\partial \eta} j + \frac{\partial T_j}{\partial y} \phi_{10j}^1 \frac{\partial y}{\partial \xi} j \\ & + \frac{\partial T_j}{\partial y} \phi_{01j}^1 \frac{\partial y}{\partial \eta} j + \frac{\partial^2 T_j}{\partial x \partial y} \left[\frac{\partial x}{\partial \eta} \frac{\partial y}{\partial \xi} j + \frac{\partial y}{\partial \eta} \frac{\partial x}{\partial \xi} j \right] \phi_{11j}^1 + \frac{\partial^2 T_j}{\partial x^2} \phi_{11j}^1 \frac{\partial x}{\partial \eta} \frac{\partial x}{\partial \xi} j \\ & + \frac{\partial^2 T_j}{\partial y^2} \phi_{11j}^1 \frac{\partial y}{\partial \eta} \frac{\partial y}{\partial \xi} j + \left[\frac{\partial T_j}{\partial x} \frac{\partial^2 x}{\partial \xi \partial \eta} j + \frac{\partial T_j}{\partial y} \frac{\partial^2 y}{\partial \xi \partial \eta} j \right] \phi_{11j}^1. \end{aligned}$$

*The superscript 1 is introduced to denote the C^1 Lagrangian Hermites.

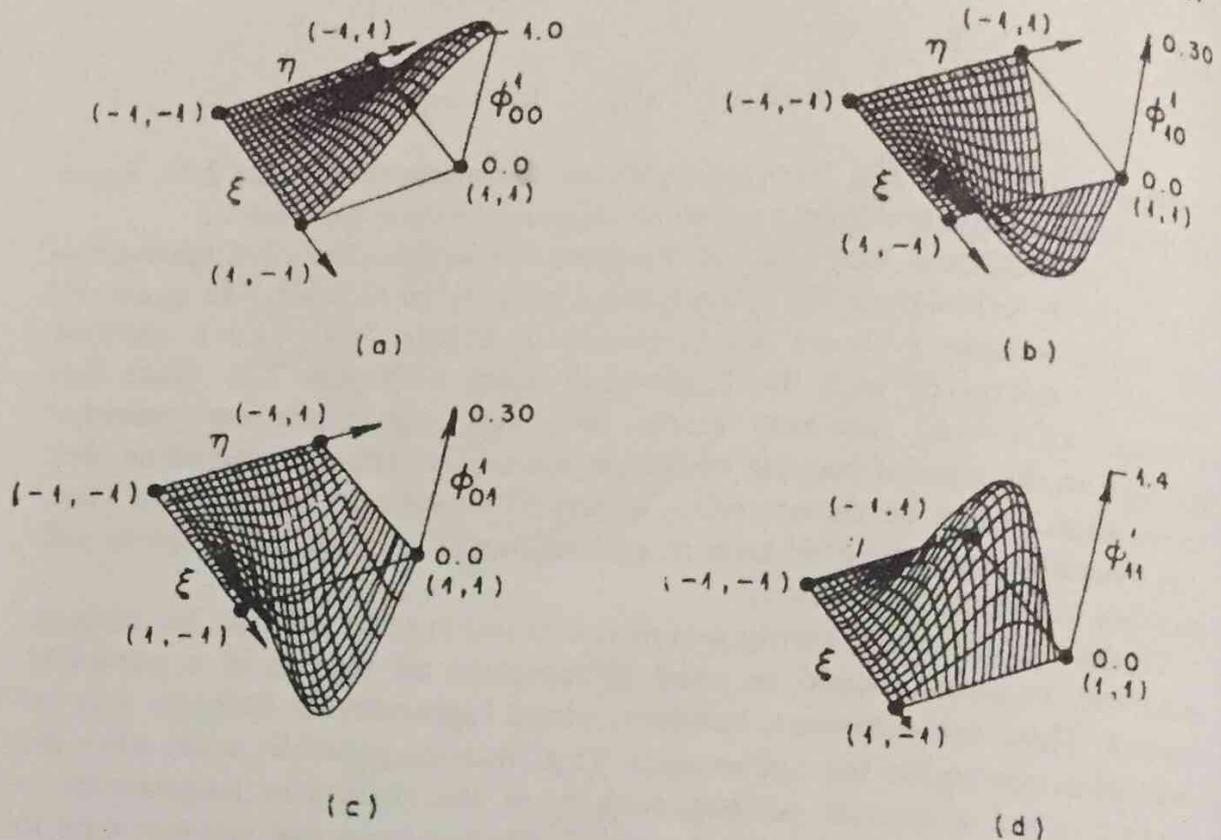


Figure 2.13. Two-dimensional basis functions formulated using Hermite polynomials.

This expansion requires four bases per node: ϕ_{00}^I , ϕ_{10}^I , ϕ_{01}^I , and ϕ_{11}^I . Their algebraic form is given in Table 2.7a and they are illustrated in Figure 2.13.

Examination of Figure 2.13 reveals that these bases manifest the following properties:

$$\frac{\partial \phi_{10}^I}{\partial \xi} \Big|_j = \frac{\partial \phi_{01}^I}{\partial \eta} \Big|_j = \frac{\partial^2 \phi_{11}^I}{\partial \xi \partial \eta} \Big|_j = 1$$

at $\xi = \xi_j, \eta = \eta_j$, the node where it is defined

and

$$\frac{\partial \phi_{10}^I}{\partial \xi} \Big|_j = \frac{\partial \phi_{01}^I}{\partial \eta} \Big|_j = \frac{\partial^2 \phi_{11}^I}{\partial \xi \partial \eta} \Big|_j = 0 \quad \text{at all other nodal locations.}$$

While (2.2.68) provides the general formulation, it is possible to rewrite this expansion in a form more clearly related to the one-dimensional expression (2.2.49). This is accomplished by defining new bases in the following way:

$$(2.2.69) \quad \hat{T} = \sum_{j=1}^4 T_j \phi_{0j}^I + \frac{\partial T_j}{\partial x} \phi_{xj}^I + \frac{\partial T_j}{\partial y} \phi_{yj}^I + \frac{\partial^2 T_j}{\partial x \partial y} \phi_{xyj}^I \\ + \frac{\partial^2 T_j}{\partial x^2} \phi_{xxj}^I + \frac{\partial^2 T_j}{\partial y^2} \phi_{yyj}^I$$

where

$$\phi_{0j}^1 = \phi_{00j}^1,$$

$$\phi_{xj}^1 = \phi_{10j}^1 \frac{\partial x}{\partial \xi} j + \phi_{01j}^1 \frac{\partial x}{\partial \eta} j + \phi_{11j}^1 \frac{\partial^2 x}{\partial \xi \partial \eta} j,$$

$$\phi_{yj}^1 = \phi_{10j}^1 \frac{\partial y}{\partial \xi} j + \phi_{01j}^1 \frac{\partial y}{\partial \eta} j + \phi_{11j}^1 \frac{\partial^2 y}{\partial \xi \partial \eta} j,$$

$$\phi_{x_{xy}j}^1 = \phi_{11j}^1 \left[\frac{\partial x}{\partial \eta} \frac{\partial y}{\partial \xi} j + \frac{\partial y}{\partial \eta} \frac{\partial x}{\partial \xi} j \right],$$

$$\phi_{x_{xx}j}^1 = \phi_{11j}^1 \frac{\partial x}{\partial \eta} \frac{\partial x}{\partial \xi} j,$$

$$\phi_{y_{yy}j}^1 = \phi_{11j}^1 \frac{\partial y}{\partial \eta} \frac{\partial y}{\partial \xi} j.$$

Comparison of (2.2.69) and (2.2.49) reveals that both are written in fundamentally the same form but with a different number of unknown parameters and bases.

In the case of zero-order continuous polynomials, we found that an incomplete polynomial could be used to formulate bases. These were designated serendipity basis functions. This approach may also be used to considerable advantage in developing two-dimensional Hermite bases. The resulting approximating expansion is

$$(2.2.70) \quad \hat{T} = \sum_{j=1}^4 T_j \phi_{00j} + \frac{\partial T_j}{\partial x} \phi_{10j} \frac{\partial x}{\partial \xi} j + \frac{\partial T_j}{\partial x} \phi_{01j} \frac{\partial x}{\partial \eta} j \\ + \frac{\partial T_j}{\partial y} \phi_{10j} \frac{\partial y}{\partial \xi} j + \frac{\partial T_j}{\partial y} \phi_{01j} \frac{\partial y}{\partial \eta} j,$$

where we have omitted the superscript 1 from the bases to emphasize that they are not first-order continuous. These bases are presented algebraically in Table 2.7a and graphically in Figure 2.14. Equation (2.2.70) may be rewritten in the form of (2.2.69) as

$$(2.2.71) \quad \hat{T} = \sum_{j=1}^4 T_j \phi_{0j} + \frac{\partial T_j}{\partial x} \phi_{xj} + \frac{\partial T_j}{\partial y} \phi_{yj},$$

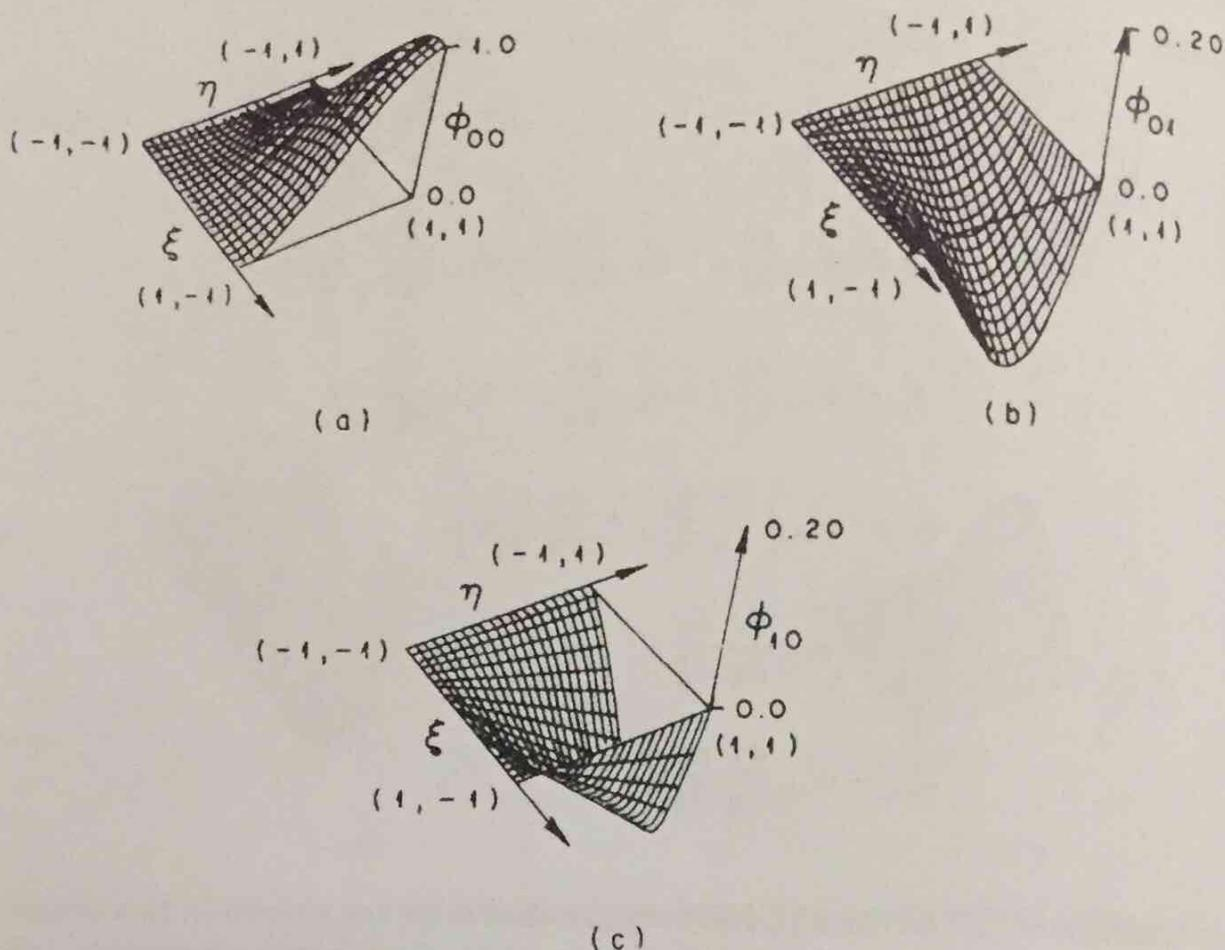


Figure 2.14. Two-dimensional serendipity basis functions formulated using Hermite polynomials.

where

$$\phi_{0j} = \phi_{00j},$$

$$\phi_{xj} = \phi_{10j} \frac{\partial x}{\partial \xi} j + \phi_{01j} \frac{\partial x}{\partial \eta} j,$$

$$\phi_{yj} = \phi_{10j} \frac{\partial y}{\partial \xi} j + \phi_{01j} \frac{\partial y}{\partial \eta} j.$$

Examination of (2.2.71) and (2.2.69) reveals a considerable saving in computational effort when serendipity rather than standard Hermitian bases are used. The degrees of freedom per node are reduced from six to three with serendipity bases. Experiments conducted using both types of bases in conjunction with the Galerkin formulation suggest that the two schemes are of comparable accuracy. The advantage of the serendipity scheme is even more pronounced in three-dimensional formulations.

2.2.5 Approximating Equations

Each of the weighted residual schemes introduced to solve the one-dimensional problem can be extended to two space dimensions. As illustrative examples, we solve the following problem using Galerkin's method with linear basis functions, and a similar problem using collocation and Hermite cubics.

Example 1

Consider the problem of two-dimensional, time-independent heat flow in a rectangular plate with a heat source located at the center of the plate. The governing equations for this problem are

$$(2.2.72a) \quad \mathcal{L}(T) \equiv T_{xx} + T_{yy} = Q,$$

$$(2.2.72b) \quad T(x, 2) = 1,$$

$$(2.2.72c) \quad T(0, y) = 1,$$

$$(2.2.72d) \quad T_y(x, 0) = 0,$$

$$(2.2.72e) \quad T_x(2, y) = 0,$$

$$(2.2.72f) \quad Q(x, y) = Q_w \delta(x-1) \delta(y-1)$$

where x and y are Cartesian coordinates, Q_w is the heat source, and δ is the Dirac delta function. The discretized domain of interest in this problem is illustrated in Figure 2.10.

Step 1

Define the trial functions

$$(2.2.73) \quad T(x, y) \approx \hat{T}(x, y) = \sum_{j=1}^9 T_j \phi_j(x, y).$$

For convenience, it is advantageous to define basis functions in local (ξ, η) coordinates whereupon (2.2.73) becomes, for *each element*,

$$(2.2.74) \quad T(x, y) \approx \hat{T}(x, y) = \sum_{j=1}^4 T_j \phi_j(\xi, \eta)$$

and $\phi_j(\xi, \eta)$ are bilinear chapeau functions such as those illustrated in Figure 2.11a.

Step 2

Formulate the integral equations using Galerkin's procedure. This is the special case of the MWR scheme wherein the weighting function has been defined as the basis function. One can also interpret Galerkin's scheme as the requirement of orthogonality between the residual R and each basis function,

$$(2.2.75) \quad \int_A R(x, y) \phi_i(x, y) dx dy = 0, \quad i = 1, \dots, 9,$$

where

$$(2.2.76) \quad R(x, y) \equiv \mathcal{L}(\hat{T}) - Q$$

and \mathcal{L} is defined by (2.2.72a). Substitution of (2.2.72a) and (2.2.76) into (2.2.75) yields

$$(2.2.77) \quad \int_A (\hat{T}_{xx} + \hat{T}_{yy} - Q) \phi_i(x, y) dx dy = 0, \quad i = 1, \dots, 9.$$

It is advantageous, but not mandatory, to apply Green's theorem to (2.2.77) to incorporate second- and third-type boundary conditions directly into the set of integral equations. Equation (2.2.77) becomes

$$(2.2.78) \quad \int_A (\hat{T}_x \phi_{xi} + \hat{T}_y \phi_{yi} + Q \phi_i) dx dy - \int_S (\hat{T}_x l_x + \hat{T}_y l_y) \phi_i ds = 0,$$

$$i = 1, \dots, 9,$$

where l_x and l_y are direction cosines with respect to the normal to the curve S , the boundary of the domain A . In this particular problem, the second term of (2.2.78) will be used to conveniently define the zero-gradient Neumann boundary conditions of (2.2.72d) and (2.2.72e).

Substitution of the trial functions, as defined by (2.2.73), into (2.2.78) yields the following set of algebraic equations:

$$(2.2.79) \quad \int_A \left(\sum_{j=1}^9 T_j (\phi_{xj} \phi_{xi} + \phi_{yj} \phi_{yi}) + Q \phi_i \right) dx dy$$

$$- \int_S (\hat{T}_x l_x + \hat{T}_y l_y) \phi_i ds = 0, \quad i = 1, \dots, 9.$$

Because ϕ_i is defined such that it is nonzero only over elements adjacent to node i (see Figure 2.10 and 2.11a) the integrations of (2.2.79) may be performed piecewise over each element and subsequently summed. Thus

(2.2.79) may be written

$$(2.2.80) \quad \sum_{e=1}^4 \int_{A_e} \left(\left(\sum_{j=1}^9 T_j (\phi_{xj} \phi_{xi} + \phi_{yj} \phi_{yi}) + Q \phi_i \right) dx dy - \int_{S_e} (\hat{T}_x l_x + \hat{T}_y l_y) \phi_i ds \right) = 0, \quad i = 1, \dots, 9,$$

where A_e is the area of element e , S_e is the curve bounding A_e , and l_α are direction cosines.

Step 3

Formulate the matrix equation. In general, it is advantageous to express (2.2.80) in terms of the local (ξ, η) coordinate system to facilitate integration (see Figure 2.15). This is easily accomplished provided that the relationship between derivatives of ϕ_j in each coordinate system is readily available. To obtain this relationship, we once again employ the chain rule to obtain

$$\frac{\partial \phi_j}{\partial \xi} = \frac{\partial \phi_j}{\partial x} \frac{\partial x}{\partial \xi} + \frac{\partial \phi_j}{\partial y} \frac{\partial y}{\partial \xi}$$

$$\frac{\partial \phi_j}{\partial \eta} = \frac{\partial \phi_j}{\partial x} \frac{\partial x}{\partial \eta} + \frac{\partial \phi_j}{\partial y} \frac{\partial y}{\partial \eta}$$

This set of equations is conveniently written in matrix form as

$$(2.2.81) \quad \begin{bmatrix} \frac{\partial \phi_j}{\partial \xi} \\ \frac{\partial \phi_j}{\partial \eta} \end{bmatrix} = \begin{bmatrix} \frac{\partial x}{\partial \xi} & \frac{\partial y}{\partial \xi} \\ \frac{\partial x}{\partial \eta} & \frac{\partial y}{\partial \eta} \end{bmatrix} \begin{bmatrix} \frac{\partial \phi_j}{\partial x} \\ \frac{\partial \phi_j}{\partial y} \end{bmatrix} \quad \text{or} \quad \begin{bmatrix} \frac{\partial \phi_j}{\partial \xi} \\ \frac{\partial \phi_j}{\partial \eta} \end{bmatrix} = [J] \begin{bmatrix} \frac{\partial \phi_j}{\partial x} \\ \frac{\partial \phi_j}{\partial y} \end{bmatrix}$$

$$\text{or} \quad \begin{bmatrix} \frac{\partial \phi_j}{\partial x} \\ \frac{\partial \phi_j}{\partial y} \end{bmatrix} = [J]^{-1} \begin{bmatrix} \frac{\partial \phi_j}{\partial \xi} \\ \frac{\partial \phi_j}{\partial \eta} \end{bmatrix},$$

where $[J]$ is the Jacobian matrix. In our example problem $[J]$ is easily evaluated as

$$(2.2.82) \quad [J] = \begin{bmatrix} 1.0 & 0.0 \\ 0.0 & 0.5 \end{bmatrix}$$

$$(2.2.83) \quad [J]^{-1} = \begin{bmatrix} 1.0 & 0.0 \\ 0.0 & 2.0 \end{bmatrix}.$$

As we shall see in the section on elements of irregular shape, the Jacobian matrix is not always this easily obtained.

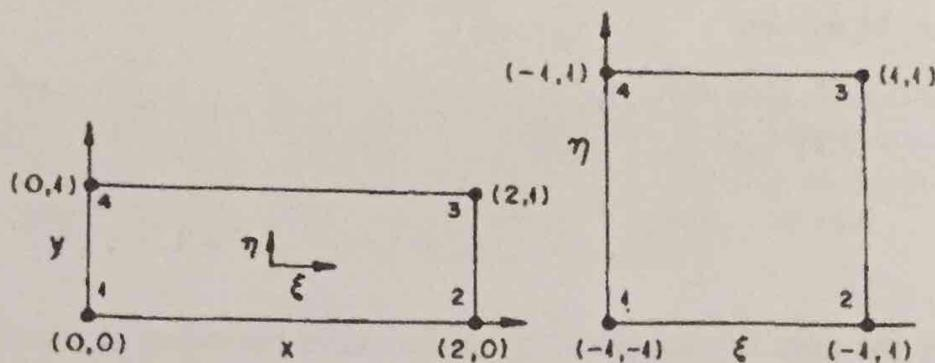


Figure 2.15. Rectangular element in (x, y) coordinates and the same element transformed into (ξ, η) coordinates.

Equations (2.2.80)–(2.2.83) may now be combined to yield the following equation defined in the local (ξ, η) coordinate system:

$$(2.2.84) \quad \sum_{e=1}^4 \left(\int_{-1}^1 \int_{-1}^1 \left(\sum_{j=1}^9 T_j (4\phi_{\xi j} \phi_{\xi i} + 4\phi_{\eta j} \phi_{\eta i}) + Q\phi_i \right) \frac{1}{4} d\xi d\eta \right. \\ \left. - \int_{S_e} (\hat{T}_x I_x + \hat{T}_y I_y) \phi_i ds \right) = 0, \quad i = 1, \dots, 9,$$

Note that in changing the limits of integration to span the local coordinate system we introduced the relationship $dx dy = \det[J] d\xi d\eta$.

Because the elements in our example problem are all of the same size, the four integrals appearing in each element in (2.2.84) are identical for each element. The assembly process, that is, the transformation from element to global integrations, is easily seen with the assistance of Table 2.8. Here we have tabulated the global nodal numbers corresponding to each element nodal number (element nodes are numbered counterclockwise from 1 to 4). For example, to find the global node corresponding to the local node 2 in element I, we move right along the second row to the column marked I, which corresponds to element I. Here a global nodal number 4 is given. Similarly, if

TABLE 2.8. Relationship between Local Node Numbers and Global Node Numbers for Problem of Figure 2.10

Element Nodes (Local Node Numbers)	Global Nodes (Global Node Numbers)			
	I	II	III	IV
1	1	2	4	5
2	4	5	7	8
3	5	6	8	9
4	2	3	5	6

TABLE 2.9. Evaluated Integrals for One Element in Local Coordinates for Equation (2.2.84)

$i \backslash j$	1	2	3	4
1	$\frac{2}{3}$	$-\frac{1}{6}$	$-\frac{1}{3}$	$-\frac{1}{6}$
2	$-\frac{1}{6}$	$\frac{2}{3}$	$-\frac{1}{6}$	$-\frac{1}{3}$
3	$-\frac{1}{3}$	$-\frac{1}{6}$	$\frac{2}{3}$	$-\frac{1}{6}$
4	$-\frac{1}{6}$	$-\frac{1}{3}$	$-\frac{1}{6}$	$\frac{2}{3}$

we wish to establish the integral values associated with global matrix coefficient $I=4$, $J=5$, the first step is to find the equivalent local numbers. Examination of Table 2.8 reveals that these two global nodal identifiers appear together in columns marked I and III. Thus these two elements (I and III) contribute information to the global integral.

The assembly procedure now calls for extracting information concerning integration at the element level from Table 2.8. From column I we see that global nodes 4 and 5 correspond to element nodes 2 and 3 in element I. Table 2.9 tells us that the contribution to the global integral attributable to these nodes is found in row 2, column 3; it is $-\frac{1}{6}$. This value is now placed in matrix location (4,5) of the global matrix. We are not through, however, because there is also information to be retrieved from element III. Table 2.8 locates this information in position (1,4) of the element matrix of Table 2.9, it is also $-\frac{1}{6}$. This value summed with the previous integral value is now placed in the same

TABLE 2.10. Evaluated Integrals for the Four Elements of Figure 2.10 in Global Coordinates for Equation (2.2.84)^a

$I \backslash J$	1	2	3	4	5	6	7	8	9
1	$\frac{2}{3}$	$-\frac{1}{6}$	0	$-\frac{1}{6}$	$-\frac{1}{3}$	0	0	0	0
2	$-\frac{1}{6}$	$\frac{4}{3}$	$-\frac{1}{6}$	$-\frac{1}{3}$	$-\frac{1}{3}$	$-\frac{1}{3}$	0	0	0
3	0	$-\frac{1}{6}$	$\frac{2}{3}$	0	$-\frac{1}{3}$	$-\frac{1}{6}$	0	0	0
4	$-\frac{1}{6}$	$-\frac{1}{3}$	0	$\frac{4}{3}$	$-\frac{1}{3}$	0	$-\frac{1}{6}$	$-\frac{1}{3}$	0
5	$-\frac{1}{3}$	$-\frac{1}{3}$	$-\frac{1}{3}$	$-\frac{1}{3}$	$\frac{8}{3}$	$-\frac{1}{3}$	$-\frac{1}{3}$	$-\frac{1}{3}$	$-\frac{1}{3}$
6	0	$-\frac{1}{3}$	$-\frac{1}{6}$	0	$-\frac{1}{3}$	$\frac{4}{3}$	0	$-\frac{1}{3}$	$-\frac{1}{6}$
7	0	0	0	$-\frac{1}{6}$	$-\frac{1}{3}$	0	$\frac{2}{3}$	$-\frac{1}{6}$	0
8	0	0	0	$-\frac{1}{3}$	$-\frac{1}{3}$	$-\frac{1}{3}$	$-\frac{1}{6}$	$\frac{4}{3}$	$-\frac{1}{6}$
9	0	0	0	0	$-\frac{1}{3}$	$-\frac{1}{6}$	0	$-\frac{1}{6}$	$\frac{2}{3}$

^aNote that these values are obtained using the information from Tables 2.8 and 2.9 only.

global matrix location (4, 5). Combination of the two integrals yields the final value of $-\frac{1}{3}$, which appears in Table 2.10 in row 4, column 5.

It is important to understand the two-step integration process outlined above, because this is the procedure used in nearly all finite element programs. In general, the element coefficient matrix (Table 2.9) is different for each element because of changes in either element geometry or parameter values. Moreover, it is often necessary to perform the integrations of (2.2.84) numerically. Because of the local coordinate system we have selected, this is easily accomplished using Gaussian quadrature (as will be outlined later). Superficially, it appears that an unnecessarily complicated procedure has been introduced to evaluate rather simple integrals. Introduction of these basic ideas at this point, however, simplifies the extension to more challenging concepts in later chapters.

Step 4

Solve the matrix equation. It is now possible, with the information of Table 2.10, to solve our example problem. The matrix equation arising out of (2.2.84) is

$$(2.2.85) \quad \begin{bmatrix} \frac{2}{3} & -\frac{1}{6} & 0 & -\frac{1}{6} & -\frac{1}{3} & 0 & 0 & 0 & 0 \\ -\frac{1}{6} & \frac{4}{3} & -\frac{1}{6} & -\frac{1}{3} & -\frac{1}{3} & -\frac{1}{3} & 0 & 0 & 0 \\ 0 & -\frac{1}{6} & \frac{2}{3} & 0 & -\frac{1}{3} & -\frac{1}{6} & 0 & 0 & 0 \\ -\frac{1}{6} & -\frac{1}{3} & 0 & \frac{4}{3} & -\frac{1}{3} & 0 & -\frac{1}{6} & -\frac{1}{3} & 0 \\ -\frac{1}{3} & -\frac{1}{3} & -\frac{1}{3} & -\frac{1}{3} & \frac{8}{3} & -\frac{1}{3} & -\frac{1}{3} & -\frac{1}{3} & -\frac{1}{3} \\ 0 & -\frac{1}{3} & -\frac{1}{6} & 0 & -\frac{1}{3} & \frac{4}{3} & 0 & -\frac{1}{3} & -\frac{1}{6} \\ 0 & 0 & 0 & -\frac{1}{6} & -\frac{1}{3} & 0 & \frac{2}{3} & -\frac{1}{6} & 0 \\ 0 & 0 & 0 & -\frac{1}{3} & -\frac{1}{3} & -\frac{1}{3} & -\frac{1}{6} & \frac{4}{3} & -\frac{1}{6} \\ 0 & 0 & 0 & 0 & -\frac{1}{3} & -\frac{1}{6} & 0 & -\frac{1}{6} & \frac{2}{3} \end{bmatrix}$$

$$\begin{bmatrix} T_1 \\ T_2 \\ T_3 \\ T_4 \\ T_5 \\ T_6 \\ T_7 \\ T_8 \\ T_9 \end{bmatrix} = \begin{bmatrix} \int_S (\hat{T}_x l_x + \hat{T}_y l_y) \phi_1 ds \\ \int_S (\hat{T}_x l_x + \hat{T}_y l_y) \phi_2 ds \\ \int_S (\hat{T}_x l_x + \hat{T}_y l_y) \phi_3 ds \\ 0 \\ -Q_w \\ \int_S (\hat{T}_x l_x + \hat{T}_y l_y) \phi_6 ds \\ 0 \\ 0 \\ \int_S (\hat{T}_x l_x + \hat{T}_y l_y) \phi_9 ds \end{bmatrix}$$

The line integrals appearing on the right-hand side of (2.2.85) represent flux boundary conditions along the perimeter of the problem area. Through summation of element integrals, these line integrals vanish along interelement boundaries. The point source becomes a value specified at node 5 through the evaluation of the Dirac delta function.

In general, when Dirichlet boundaries are specified, it is necessary to expand and evaluate the line integrals. However, when C^0 bases are used, one can condense rows containing the known temperature values out of the matrix equation. Rows 1, 2, 3, 6, and 9 may thus be eliminated. The corresponding columns may also be eliminated by placing information pertaining to these nodes on the right-hand side of equations 4, 5, 7, and 8. The reduced matrix equation is

$$(2.2.86) \quad \begin{bmatrix} \frac{4}{3} & -\frac{1}{3} & -\frac{1}{6} & -\frac{1}{3} \\ -\frac{1}{3} & \frac{8}{3} & -\frac{1}{3} & -\frac{1}{3} \\ -\frac{1}{6} & -\frac{1}{3} & \frac{2}{3} & -\frac{1}{6} \\ -\frac{1}{3} & -\frac{1}{3} & -\frac{1}{6} & \frac{4}{3} \end{bmatrix} \begin{bmatrix} T_4 \\ T_5 \\ T_7 \\ T_8 \end{bmatrix} = \begin{bmatrix} \frac{1}{2} \\ -Q_w + \frac{2}{3} \\ 0 \\ \frac{1}{2} \end{bmatrix}$$

or

$$(2.2.87) \quad [A]\{b\} = \{f\}.$$

Equation (2.2.87) may be solved directly to yield

$$\begin{bmatrix} T_4 \\ T_5 \\ T_7 \\ T_8 \end{bmatrix} = \begin{bmatrix} 0.783 \\ 0.525 \\ 0.655 \\ 0.783 \end{bmatrix}.$$

The coefficients T_4 , T_5 , T_7 , and T_8 represent the values of the temperature at nodes 4, 5, 7, and 8 because the basis functions are defined such that ϕ_i is unity at node i and zero elsewhere.

The analytical solution for this problem is (Tang, 1979)

$$T = U + V + W,$$

where

$$U = \frac{2}{\pi} \sum_{n=0}^{\infty} \frac{\sin[(n + \frac{1}{2})\pi(a - y)/a] \cosh[(n + \frac{1}{2})\pi(a - x)/a]}{(n + \frac{1}{2}) \cosh(n + \frac{1}{2})\pi}$$

$$V = \frac{2}{\pi} \sum_{n=0}^{\infty} \frac{\cosh[(n + \frac{1}{2})\pi y/a] \sin[(n + \frac{1}{2})\pi x/a]}{(n + \frac{1}{2}) \cosh(n + \frac{1}{2})\pi}$$

$$W = \frac{2}{\pi} \sum_{n=0}^{\infty} \frac{\sin[(n + \frac{1}{2})\pi x/a] \sin[(n + \frac{1}{2})\pi \xi/a] \cdot \sinh[(n + \frac{1}{2})\pi(a - y)/a] \cosh[(n + \frac{1}{2})\pi \eta/a]}{(n + \frac{1}{2}) \cosh[(n + \frac{1}{2})\pi]}.$$

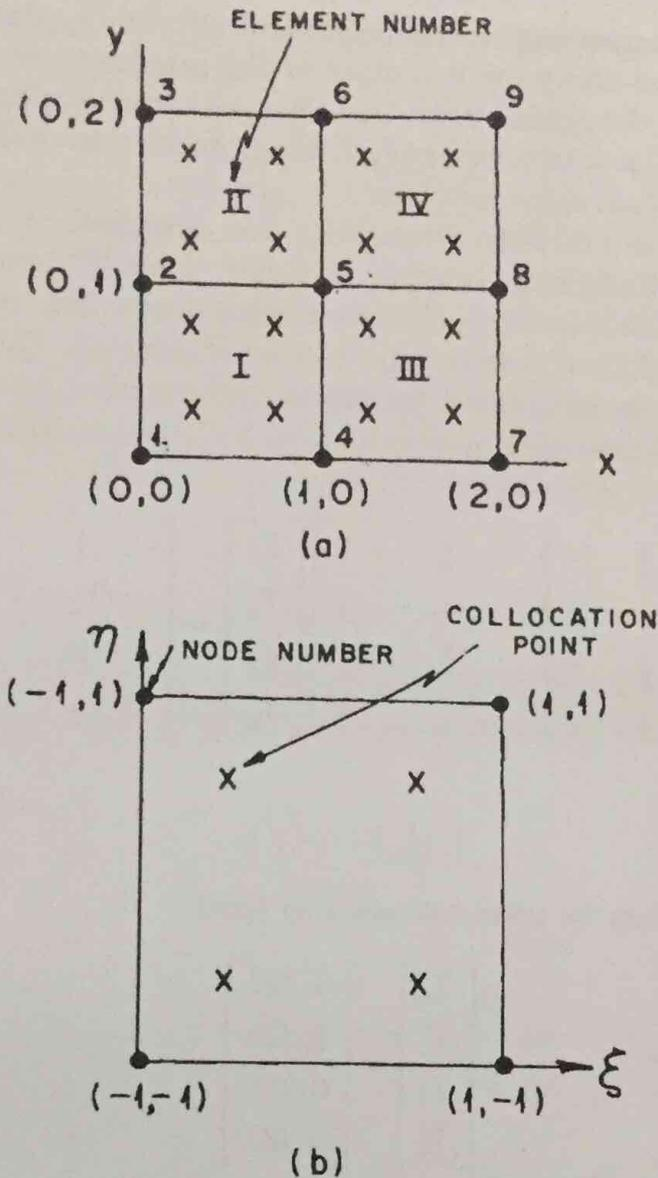


Figure 2.16. (a) Collocation net in (x, y) coordinates. (b) One element of collocation net in (ξ, η) coordinates.

where a is the length of the side of the square ($a = 2$), and ξ and η are the x and y locations of the heat source, respectively. The analytical solution for the nodal locations 4, 5, 7, and 8 is 0.756, 0.127, 0.719, and 0.756, respectively. It is evident that the numerical solution at the singular point $(1, 1)$ is not very accurate. This is not unusual inasmuch as we are attempting to represent a rapidly varying function with four bilinear elements. We will see in Chapter 4 that special trial functions can be used to circumvent this difficulty.

Example 2*

In this example we consider the solution of Laplace's equation on a square region using the collocation method. The problem is illustrated in Figure 2.16

*The calculations for this example were made by Michael Celia, a research assistant in the Department of Civil Engineering, Princeton University.

and the governing equations follow:

$$(2.2.88a) \quad \mathcal{L}_0(u) = u_{xx} + u_{yy} = 0,$$

$$(2.2.88b) \quad u_x(0, y) = 0, \quad 0 < y < 2,$$

$$(2.2.88c) \quad u_x(2, y) = 0, \quad 0 < y < 2,$$

$$(2.2.88d) \quad u(x, 0) = 3 - x, \quad 0 < x < 2,$$

$$(2.2.88e) \quad u(x, 2) = 3 - x, \quad 0 < x < 2,$$

where u may have a number of physical interpretations such as electrical potential, temperature, or hydraulic head.

Step 1

Define the trial functions. In this case we use cubic Hermite polynomials as basis functions. Thus the trial function for each element is written [see (2.2.69)]*

$$(2.2.89) \quad u(x, y) \approx \hat{u}(x, y) = \sum_{j=1}^4 U_j \phi_{0j}^1 + \frac{\partial U_j}{\partial x} \phi_{xj}^1 + \frac{\partial U_j}{\partial y} \phi_{yj}^1 \\ + \frac{\partial^2 U_j}{\partial x \partial y} \phi_{xyj}^1 + \frac{\partial^2 U_j}{\partial x^2} \phi_{xxj}^1 + \frac{\partial^2 U_j}{\partial y^2} \phi_{yyj}^1,$$

where

$$\phi_{0j}^1 = \phi_{00j}^1,$$

$$\phi_{xj}^1 = \phi_{10j}^1 \frac{\partial x}{\partial \xi} j + \phi_{01j}^1 \frac{\partial x}{\partial \eta} j + \phi_{11j}^1 \frac{\partial^2 x}{\partial \xi \partial \eta} j,$$

$$\phi_{yj}^1 = \phi_{10j}^1 \frac{\partial y}{\partial \xi} j + \phi_{01j}^1 \frac{\partial y}{\partial \eta} j + \phi_{11j}^1 \frac{\partial^2 y}{\partial \xi \partial \eta} j,$$

$$\phi_{xyj}^1 = \phi_{11j}^1 \left[\frac{\partial x}{\partial \eta} \frac{\partial y}{\partial \xi} j + \frac{\partial y}{\partial \eta} \frac{\partial x}{\partial \xi} j \right],$$

$$\phi_{xxj}^1 = \phi_{11j}^1 \frac{\partial x}{\partial \eta} \frac{\partial x}{\partial \xi} j,$$

$$\phi_{yyj}^1 = \phi_{11j}^1 \frac{\partial y}{\partial \eta} \frac{\partial y}{\partial \xi} j.$$

*Note that the x and y subscripts do not denote partial derivatives in this equation.

Because we are using square elements in this example, $\partial x / \partial \eta = \partial y / \partial \xi = 0$, and the following simplifications are possible:

$$(2.2.90) \quad \phi_{xxj}^I = \phi_{yyj}^I = 0, \quad \phi_{xj}^I = \phi_{10j}^I \frac{\partial x}{\partial \xi} j,$$

$$\phi_{xyj}^I = \phi_{11j}^I \frac{\partial y}{\partial \eta} \frac{\partial x}{\partial \xi} j, \quad \phi_{yj}^I = \phi_{01j}^I \frac{\partial y}{\partial \eta} j.$$

Combination of (2.2.90) with (2.2.89) yields the appropriate trial function for a single element:

$$(2.2.91) \quad u(x, y) \approx \hat{u}(x, y) = \sum_{j=1}^4 U_j \phi_{00j}^I + \frac{\partial U_j}{\partial x} \phi_{10j}^I \frac{\partial x}{\partial \xi} j + \frac{\partial U_j}{\partial y} \phi_{01j}^I \frac{\partial y}{\partial \eta} j$$

$$+ \frac{\partial^2 U_j}{\partial x \partial y} \phi_{11j}^I \frac{\partial y}{\partial \eta} \frac{\partial x}{\partial \xi} j.$$

It can be seen through a comparison of Figure 2.16a and b that $\partial x / \partial \xi = \partial y / \partial \eta = \frac{1}{2}$ in this particular example.

Step 2

Formulate the approximating algorithm using the collocation procedure. In this case of the MWR, the weighting function is chosen to be the Dirac delta function specified at the 16 Gauss points (x_i, y_i) . Thus we obtain

$$(2.2.92) \quad \int_x \int_y R(x, y) \delta(x - x_i, y - y_i) dy dx = 0, \quad i = 1, 2, \dots, 16,$$

where $R(x, y)$ is the residual defined as

$$(2.2.93) \quad R(x, y) \equiv \mathcal{L}_0(\hat{u})$$

and $\mathcal{L}_0(\cdot)$ is defined in (2.2.88a). Substitution of (2.2.93) into (2.2.92) yields

$$(2.2.94) \quad \int_x \int_y \mathcal{L}_0(\hat{u}) \delta(x - x_i, y - y_i) dy dx = 0, \quad i = 1, 2, \dots, 16.$$

We now transform (2.2.94) from (x, y) to (ξ, η) space, not because it is particularly valuable in this example, but rather to provide a foundation for more complex formulations to follow in later sections. In (ξ, η) coordinates

(2.2.94) becomes, for each element,

$$(2.2.95) \quad \int_{\xi} \int_{\eta} \mathcal{L}_0(\hat{u}) \delta(\xi - \xi_k, \eta - \eta_k) \det[J] d\eta d\xi = 0, \quad k = 1, 2, \dots, 4,$$

where $[J]$ is the Jacobian matrix of (2.2.81). Let us now substitute for the operator $\mathcal{L}_0(\hat{u})$ in (2.2.95):

(2.2.96)

$$\int_{\xi} \int_{\eta} (\hat{u}_{xx} + \hat{u}_{yy}) \delta(\xi - \xi_k, \eta - \eta_k) \det[J] d\eta d\xi = 0, \quad k = 1, 2, \dots, 4.$$

From the definition of the Dirac delta function, we can rewrite (2.2.96) as

$$(2.2.97) \quad (\hat{u}_{xx} + \hat{u}_{yy}) \det[J] \Big|_{\xi_k, \eta_k} = 0, \quad k = 1, 2, \dots, 4,$$

where (ξ_k, η_k) is the coordinate of the k th Gauss point.

Introduction of the definition of the trial function (2.2.91) into the collocation expression (2.2.97) yields, in a given element,

$$(2.2.98) \quad \left[\left\{ \sum_{j=1}^4 \left(U_j \frac{\partial^2}{\partial x^2} \phi_{00j}^1 + \frac{\partial U_j}{\partial x} \frac{\partial x}{\partial \xi} j \frac{\partial^2}{\partial x^2} \phi_{10j}^1 + \frac{\partial U_j}{\partial y} \frac{\partial y}{\partial \eta} j \frac{\partial^2}{\partial x^2} \phi_{01j}^1 \right. \right. \right. \\ \left. \left. + \frac{\partial^2 U_j}{\partial x \partial y} \frac{\partial y}{\partial \eta} \frac{\partial x}{\partial \xi} j \frac{\partial^2}{\partial x^2} \phi_{11j}^1 \right) + \left(U_j \frac{\partial^2}{\partial y^2} \phi_{00j}^1 + \frac{\partial U_j}{\partial x} \frac{\partial x}{\partial \xi} j \frac{\partial^2}{\partial y^2} \phi_{10j}^1 \right. \right. \\ \left. \left. + \frac{\partial U_j}{\partial y} \frac{\partial y}{\partial \eta} j \frac{\partial^2}{\partial y^2} \phi_{01j}^1 + \frac{\partial^2 U_j}{\partial x \partial y} \frac{\partial y}{\partial \eta} \frac{\partial x}{\partial \xi} j \frac{\partial^2}{\partial y^2} \phi_{11j}^1 \right) \right\} \det[J] \Big|_{\xi_k, \eta_k} = 0, \\ k = 1, 2, \dots, 4.$$

Step 3

Formulate the matrix equation. To evaluate (2.2.97) we must calculate the determinant of the Jacobian matrix and establish a transformation for the second-order derivatives from the (x, y) to the (ξ, η) coordinate system. The Jacobian is obtained directly from the definitions of $\partial x / \partial \xi$ and $\partial y / \partial \eta$, which are observed to be $\frac{1}{2}$ from Figure 2.16, as mentioned earlier. Thus we

obtain

$$(2.2.99) \quad \det[J] = \begin{vmatrix} \frac{\partial x}{\partial \xi} & \frac{\partial y}{\partial \xi} \\ \frac{\partial x}{\partial \eta} & \frac{\partial y}{\partial \eta} \end{vmatrix} = \begin{vmatrix} \frac{1}{2} & 0 \\ 0 & \frac{1}{2} \end{vmatrix} = \frac{1}{4}.$$

To transform the derivatives, we once again use the chain rule expansion
(2.2.100)

$$\begin{aligned} \frac{\partial^2 \phi}{\partial x^2} &= \frac{\partial}{\partial x} \left(\frac{\partial \phi}{\partial x} \right) \\ &= \frac{\partial}{\partial x} \left(\frac{\partial \phi}{\partial \xi} \frac{\partial \xi}{\partial x} + \frac{\partial \phi}{\partial \eta} \frac{\partial \eta}{\partial x} \right) = \left(\frac{\partial \xi}{\partial x} \frac{\partial}{\partial \xi} + \frac{\partial \eta}{\partial x} \frac{\partial}{\partial \eta} \right) \left(\frac{\partial \phi}{\partial \xi} \frac{\partial \xi}{\partial x} + \frac{\partial \phi}{\partial \eta} \frac{\partial \eta}{\partial x} \right) \\ &= \left(\frac{\partial \xi}{\partial x} \right)^2 \frac{\partial^2 \phi}{\partial \xi^2} + 2 \frac{\partial \xi}{\partial x} \frac{\partial \eta}{\partial x} \frac{\partial^2 \phi}{\partial \xi \partial \eta} + \left(\frac{\partial \eta}{\partial x} \right)^2 \frac{\partial^2 \phi}{\partial \eta^2} \\ &\quad + \frac{\partial^2 \xi}{\partial x^2} \frac{\partial \phi}{\partial \xi} + \frac{\partial^2 \eta}{\partial x^2} \frac{\partial \phi}{\partial \eta}. \end{aligned}$$

Because of the geometry, this particular problem (2.2.100) reduces to

$$(2.2.101a) \quad \frac{\partial^2 \phi}{\partial x^2} = \frac{\partial^2 \phi}{\partial \xi^2} \left(\frac{\partial \xi}{\partial x} \right)^2 = \frac{\partial^2 \phi}{\partial \xi^2} (4),$$

and similarly

$$(2.2.101b) \quad \frac{\partial^2 \phi}{\partial y^2} = \frac{\partial^2 \phi}{\partial \eta^2} \left(\frac{\partial \eta}{\partial y} \right)^2 = \frac{\partial^2 \phi}{\partial \eta^2} (4).$$

The final equation to be evaluated at each collocation point is obtained by substitution of (2.2.101) and (2.2.99) into (2.2.98):

(2.2.102)

$$\left\{ \sum_{j=1}^4 \left(U_j \frac{\partial^2}{\partial \xi^2} \phi_{00,j}^1 + \frac{1}{2} \frac{\partial U_j}{\partial x} \frac{\partial^2}{\partial \xi^2} \phi_{10,j}^1 + \frac{1}{2} \frac{\partial U_j}{\partial y} \frac{\partial^2}{\partial \xi^2} \phi_{01,j}^1 + \frac{1}{4} \frac{\partial^2 U_j}{\partial x \partial y} \frac{\partial^2}{\partial \xi^2} \phi_{11,j}^1 \right) + \left(U_j \frac{\partial^2}{\partial \eta^2} \phi_{00,j}^1 + \frac{1}{2} \frac{\partial U_j}{\partial x} \frac{\partial^2}{\partial \eta^2} \phi_{10,j}^1 + \frac{1}{2} \frac{\partial U_j}{\partial y} \frac{\partial^2}{\partial \eta^2} \phi_{01,j}^1 + \frac{1}{4} \frac{\partial^2 U_j}{\partial x \partial y} \frac{\partial^2}{\partial \eta^2} \phi_{11,j}^1 \right) \right\} \Big|_{\xi_k, \eta_k} = 0, \quad k = 1, 2, \dots, 4.$$

It is important to recognize that (2.2.102) is written for one element only. It contains 16 unknowns while generating only four equations. When this equation is evaluated for all four elements, we will have 16 equations, but there will now be 36 unknowns. However, the number of unknowns will reduce to 16 when the appropriate boundary conditions are imposed.

Step 4

Solve the algebraic equations. To solve the algebraic equations associated with (2.2.102), we first evaluate this equation for each element. The resulting element equations are

$$(2.2.103) \quad \begin{bmatrix} H_{11} & H_{12} & H_{13} & H_{14} \\ H_{21} & H_{22} & H_{23} & H_{24} \\ H_{31} & H_{32} & H_{33} & H_{34} \\ H_{41} & H_{42} & H_{43} & H_{44} \end{bmatrix} \begin{bmatrix} X_1 \\ X_2 \\ X_3 \\ X_4 \end{bmatrix} = 0$$

or

$$[H]\{x\} = 0,$$

where the elements of $[H]$ and $\{x\}$ are row and column vectors, respectively, that is,

$$H_{k,j} = \left[\left(\frac{\partial^2}{\partial \xi^2} + \frac{\partial^2}{\partial \eta^2} \right) \phi_{00j}^I, \frac{1}{2} \left(\frac{\partial^2}{\partial \xi^2} + \frac{\partial^2}{\partial \eta^2} \right) \phi_{10j}^I, \right. \\ \left. \frac{1}{2} \left(\frac{\partial^2}{\partial \xi^2} + \frac{\partial^2}{\partial \eta^2} \right) \phi_{01j}^I, \frac{1}{4} \left(\frac{\partial^2}{\partial \xi^2} + \frac{\partial^2}{\partial \eta^2} \right) \phi_{11j}^I \right] \Big|_{\xi_k, \eta_k}$$

$$X_j = \left[U_j, \frac{\partial U_j}{\partial x}, \frac{\partial U_j}{\partial y}, \frac{\partial^2 U_j}{\partial x \partial y} \right]^T.$$

It should be noted that $[H]$ is not a square matrix inasmuch as there are only four collocation points ($k = 1, 2, 3, 4$) and 16 undetermined coefficients in $\{x\}$.

Once the element coefficient matrix $[H]$ is generated for each element, we must assemble this information into a global matrix. We recognize that many of the undetermined parameters in $\{x\}$ are common to two or more finite elements. This assembly process generates a (16×36) global coefficient matrix. The associated global vector of unknowns is

$$2.2.104) \quad \{G\} = [\{g\}_1, \{g\}_2, \{g\}_3, \dots, \{g\}_9]^T,$$

where

$$\{g\}_m = \left[U_m, \frac{\partial U_m}{\partial x}, \frac{\partial U_m}{\partial y}, \frac{\partial^2 U_m}{\partial x \partial y} \right]^T.$$

To obtain a tractable set of equations, we impose the four boundary conditions specified in (2.2.88). This reduces the number of unknowns to 32. It is possible, however, to extract additional information from the boundary conditions. For example, because $u_x = 0$ along the side defined by $x=0$, the cross derivative $\partial/\partial y$ ($\partial/\partial x$) must also vanish along this side. Thus we have generated an additional constraint on the global system of equations. Similar arguments lead to the following additional constraints:

$$(2.2.105a) \quad \frac{\partial U_j}{\partial x} = -1, \quad j=4,6,$$

$$(2.2.105b) \quad \frac{\partial^2 U_j}{\partial x \partial y} = 0, \quad j=1,2,3,7,8,9.$$

We now have a total of 20 constraints (see Figure 2.17), 16 degrees of freedom, and a tractable system of equations. The solution to this set of equations and a comparison with the analytical solution is given in Table 2.11. Because the corner nodes are singular in terms of $\partial u/\partial x$, an alternative set of constraints, in which $\partial U_j/\partial x = -1$, $j=1,3,7,9$, is also possible. In this case, however, it is more difficult to argue the disappearance of the cross derivative.

Before leaving this introduction to the fundamental concepts underlying the finite element method, let us consider briefly the relationship between finite element and finite difference methods.

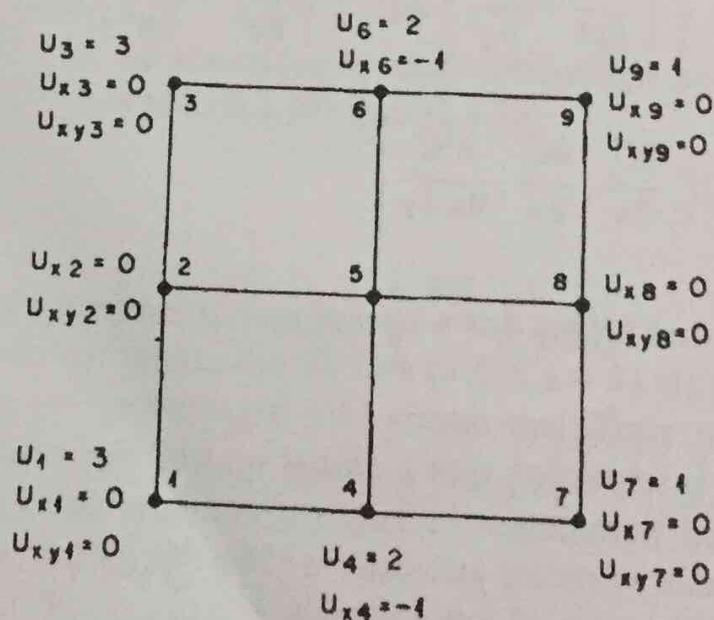


Figure 2.17. Dependent variable constraints for the collocation formulation using Hermite polynomial bases.

TABLE 2.11. Collocation and Analytical Solutions for Problem Described by Equation (2.2.88) and Illustrated in Figure 2.17

Dependent Variable	Collocation Solution	Analytical Solution	Percentage Error
U_{y1}	-1.553		
U_2	2.384	2.325	2.5
U_{v2}	8.325×10^{-16}	0.0000	0.0
U_{v3}	1.553		
U_{v4}	3.322×10^{-16}	0.0000	0.0
U_{xv4}	5.427×10^{-2}		
U_5	1.999	2.000	0.0
U_{x5}	-5.715×10^{-1}	-0.5000	14
U_{v5}	-8.240×10^{-17}	0.0000	0.0
U_{xv5}	-1.256×10^{-15}		
U_{v6}	1.474×10^{-16}	0.0000	0.0
U_{xv6}	-5.427×10^{-2}		
U_{v7}	1.553		
U_8	1.616	1.675	3.5
U_{v8}	7.372×10^{-17}	0.0000	0.0
U_{v9}	-1.553		

2.3 RELATIONSHIP BETWEEN FINITE ELEMENT AND FINITE DIFFERENCE METHODS

In Sections 2.2.1 and 2.2.2 we considered the relationships between the various weighted residual approximations. Let us now compare the finite element and finite difference methods to establish whether there are any features common to both.

Consider once again the two-dimensional heat flow problem of the preceding section, but with the nodes renumbered as illustrated in Figure 2.18. Because node (0,0) is interior to the domain, the equation associated with that node can be used to demonstrate the general form of the finite element approximation. In other words, row 5 of the coefficient matrix of (2.2.85) does not reflect the influence of boundary conditions imposed on the system. When this row of the matrix equation is expanded, the resulting equation is

$$(2.3.1) \quad \frac{1}{3}(T_{-1,-1} + T_{-1,0} + T_{-1,1} + T_{0,-1} - 8T_{0,0} + T_{0,1} + T_{1,-1} + T_{1,0} + T_{1,1}) = Q_w.$$

Although this expression cannot be readily interpreted in terms of standard finite difference notation, it can be rearranged to make the relationship more